Understanding the mechanism of non-polar Diels–Alder reactions. A comparative ELF analysis of concerted and stepwise diradical mechanisms†

Luis R. Domingo,*[a] Eduardo Chamorro[b] and Patricia Pérez[b]

Received 10th August 2010, Accepted 10th September 2010
DOI: 10.1039/c0ob00563k

The electron-reorganization along the concerted and stepwise pathways associated with the non-polar Diels–Alder reaction between cyclopentadiene (Cp, **1**) and ethylene (**2**) has been studied using the topological analysis of the electron localization function (ELF) at the B3LYP/6-31G(d) level of theory. ELF results for the concerted mechanism stresses that the electron-reorganization demanded on the diene and ethylene reagents to reach two *pseudo-diradical* structures is responsible for the high activation energy. A comparative ELF analysis of some relevant points of the non-polar Diels–Alder reaction between Cp and styrene (**10**) suggests that these concerted mechanisms do not have a *pericyclic* electron-reorganization.

Introduction

The Diels–Alder (DA) reaction is arguably one of the most powerful reactions in the arsenal of the synthetic organic chemist.[1] By varying the nature of the diene and dienophile, many different types of carbocyclic structures can be built. From the discovery of the DA reaction in the 1920s by Otto Diels and Kurt Alder,[2] a tremendous amount of experimental and theoretical work has been devoted to the study of the mechanism and the selectivity of these cycloadditions reactions. Several theories and rules have been proposed in the literature for the study of the reactivity and selectivity of cycloadditions, namely the frontier molecular orbital (FMO) theory,[3] the transition state theory (TST),[4] and more recently static reactivity indexes defined within the conceptual density functional theory (DFT).[5]

An exhaustive study of DA reactions involving different substitutions at the diene and dienophile has allowed for a rationalization of the main factor responsible for the activation energy of DA reactions. A good correlation between the activation energy and the polar character of the DA reaction measured as the charge transfer (CT) at the transition state (TS) structure has been found.[6] This finding allowed for the establishment of the polar mechanism, which is characterized by electrophilic/nucleophilic interactions at the TS. This finding has made it possible to establish classification of DA reactions as non-polar DA reactions, characterized by high activation energies, and polar DA reactions, with low activation energies (see Scheme 1). Note that ionic DA reactions, case c in Scheme 1, are an extreme case of the polar DA reaction, in which one of the two reagents is a cationic species.[6]

The prototype of non-polar DA reactions is the butadiene **8**/ethylene **2** reaction (see Scheme 2). This DA reaction must be forced to take place after 17 h at 165° C and at 900 atmospheres, giving a 78% yield. From the discovery of this reaction, the interest in the mechanism of the butadiene **8**/ethylene **2** DA reaction has stimulated a large number of theoretical studies in the last 70 years.[7] Two limiting mechanisms have been proposed: (i) a concerted mechanism, in which the two new bonds are symmetrically formed, and (ii) a stepwise mechanism *via* formation of a diradical intermediate (see Scheme 2).[7] The analysis of the activation energies involved in these mechanisms using the TST at different quantum chemical levels has estimated that the activation

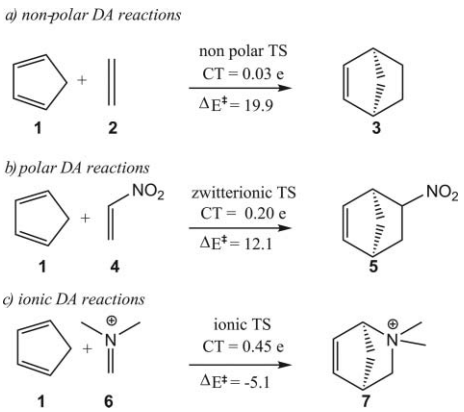

Scheme 1 Classification of Diels–Alder reactions

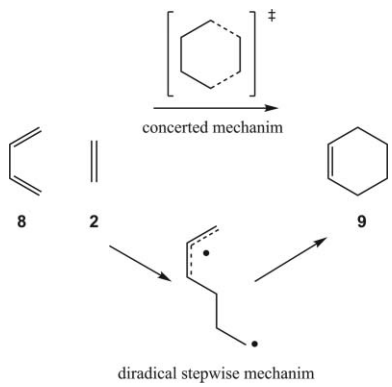

Scheme 2

[a]*Universidad de Valencia, Departamento de Química Orgánica, Dr Moliner 50, E-46100 Burjassot, Valencia, Spain. E-mail: domingo@utopia.uv.es; Fax: (+34) 96 354 4328*
[b]*Universidad Andres Bello, Departamento de Ciencias Químicas, Facultad de Ecología y Recursos Naturales, Laboratorio de Química Teórica, Av. República 275, 8370146, Santiago, Chile*

† Electronic supplementary information (ESI) available: (U)B3LYP/6-31G* computed total energies, unique frequency imaginary, and cartesian coordinates of the stationary points involved in the non-polar Diels–Alder reactions of cyclopentadiene **1** with ethylene **2** and styrene **10**. See DOI: 10.1039/c0ob00563k

energy associated with the formation of the diradical intermediate is 2.3–7.7 kcal mol^{-1} higher than that for the concerted mechanism, being in good agreement with the experimental estimates of 2–7 kcal mol^{-1}.[7b]

The first TS for the concerted DA reaction between butadiene **8**/ethylene **2** was proposed by A. Wassermann in 1935.[8] It was suggested that the lengths of the two forming bonds in the symmetric TS were 2.0 Å, a distance close to the 2.2 Å currently obtained. Today, this concerted TS is utilized as a prototype for concerted DA reactions in all textbooks. During the period from 1965 to 1969 R. B. Woodward and R. Hoffmann developed the concept of *pericyclic* reactions.[9] They defined *pericyclic* reactions as "*reactions in which all first order changing in bonding relationship take place in concert on a close curve*".[9] They uncovered the principles of orbital symmetry conservation, according to which allowed reactions could be concerted and forbidden ones could not. The importance of the symmetry of frontier orbitals in *pericyclic* reactions was discovered by K. Fukui, who made the fundamental assumption that a majority of chemical reactions should take place at the position and the direction of maximum overlapping of the HOMO and the LUMO frontier orbital of the reacting species.[3] The orbital symmetry together the FMO theory provided theoretical backing to the notion that *pericyclic* reactions occur by means of a concerted mechanism.

Recently, the non-polar DA butadiene **8**/ethylene **2** reaction has been revised using the bonding evolution theory,[10] consisting of the joint use of electron localization function (ELF)[11] and the Thom's catastrophe theory,[12] in order to characterize the changes of bonding along the reaction coordinate.[13] Interestingly, the changes in electron density going to the concerted TS are ordered to break the three π bonds present in butadiene **8** and ethylene **2** frameworks. Only after passing the TS geometry ($D = 2.27$ Å), and a distance of $D = 2.15$ Å, four monosynaptic basins appear, which collapse at 2.04 Å to create the two new σ bonds (see structures *a* and *b* in Fig. 1).[13] The analysis of the ELF suggests that the high activation energy associated with these non-polar DA reactions is mainly associated with the break of the three π bonds required to reach the TS structure.[14] A main conclusion can be redrawn from this study: the ELF analysis of the electron-reorganization along the reaction coordinates for the DA reaction between butadiene **8** and ethylene **2** indicates that *the reaction does not follow a cyclic electron-rearrangement and, in consequence, the pericyclic model does not account for the changes in bond breaking/formation for the concerted mechanism*. Note that polar DA reactions involving asymmetric reagents take place through highly asymmetric TSs characterized by nucleophilic/electrophilic interactions and, in consequence, neither obeys the *pericyclic* model.[6]

In view that structure (b) has a double biradical character as a consequence of the non-bonding electron-density concentrated at the terminal carbon atoms of the butadiene and ethylene systems, it is possible that the electronic changes along the concerted and stepwise mechanisms are not much different. To probe this assumption, the concerted and stepwise reaction pathways associated with the non-polar DA reaction between Cp **1** and ethylene **2** are analyzed in this work using the ELF methodology (see Scheme 3). The similarity of the electron-reorganization of both mechanisms will be stated by comparative ELF analysis of the most relevant points for the asynchronous one-step and the stepwise mechanisms associated with the DA reaction between Cp **1** and styrene **10** (see Scheme 4).

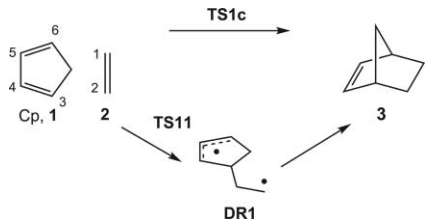

Scheme 3 One-step and stepwise pathways of the Diels–Alder reaction between cyclopentadiene Cp **1** and ethylene **2**

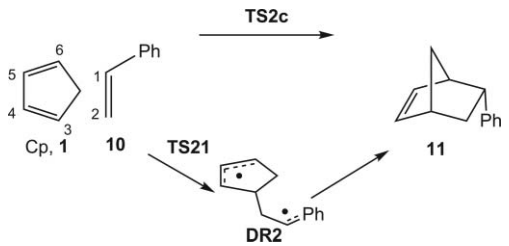

Scheme 4 One-step and stepwise pathways of the Diels–Alder reaction between cyclopentadiene Cp **1** and styrene **10**

Results and discussion

(a) Study of non-polar DA reactions between Cp 1 and ethylene 2, and Cp 1 and styrene 10

The DA reaction between Cp **1** and ethylene **2** with formation of the cycloadduct (CA) **3** has two different mechanisms: (i) a

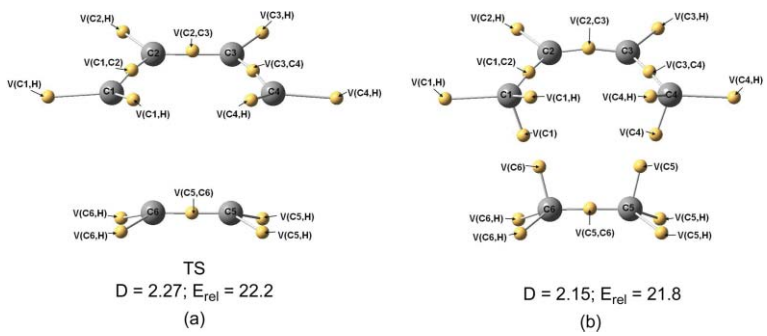

Fig. 1 Spatial localization of the maximum (*e.g.* attractors) of the ELF for relevant points on the IRC for the DA reaction between butadiene **8** and ethylene **2**. Distances D are given in Angstroms and relative energies, E_{rel}, are given in kcal mol^{-1}.

Table 1 (U)B3LYP/6-31G(d) total (E, in au) and relative (ΔE, in kcal mol^{-1}) energies involved in the non-polar DA reactions between cyclopentadiene **1** and ethylene **2** or styrene **10**

	E	ΔE
1	−194.101059	
2	−78.587457	
TS1c	−272.656774	19.9
TS11	−272.633098	34.8
DR1	−272.642138	29.1
3	−272.727426	−24.4
10	−309.648259	
TS2c	−503.716310	20.7
TS21	−503.704339	28.2
DR2	−503.717227	20.1
11	−503.776345	−17.0

one-step mechanism *via* the symmetric concerted **TS1c**, and (ii) a stepwise mechanism with formation of diradical intermediate **DR1** (see Scheme 3). These mechanisms could be characterized by the C1–C2–C3–C4 α dihedral angle. In the one-step mechanism, the α angle of *ca.* 60 degrees favors concerted C–C bond-formations since it allows for the simultaneous approach of the C1 and C2 carbon atoms of ethylene **2**, towards the C3 and C6 terminal carbon of the conjugate system of Cp **1**. In the first part of the stepwise mechanism, the α angle is *ca.* −60 degrees. This rearrangement causes the C1 and C6 carbons to be distant, and it does not permit the formation of the second σ bond in a single step. Along the reaction coordinates for the stepwise mechanism, the formation of the diradical intermediate **DR1** is achieved along C2–C3 bond formation *via* **TS11**. Formation of the second C1–C6 bond requires a C2–C3 bond rotation in the intermediate **DR1** in order to approach the C1 and C6 carbons.[7b] The second step does not have an appreciable barrier, and consequently it has not been considered.

The activation barriers associated with the concerted and stepwise DA reaction between Cp **1** and ethylene **2** are 19.9 (**TS1c**) and 34.8 (**TS11**) kcal mol^{-1}, respectively (see Table 1). Consequently, the stepwise mechanism *via* **TS11** is 15 kcal mol^{-1} more unfavorable than the concerted mechanism *via* **TS1c**. This high-energy difference makes it possible to rule out the cycloaddition through the diradical intermediate **DR1**, which is located 29.1 kcal mol^{-1} above the separated reagents. Formation of CA **3** is exothermic by −24.4 kcal mol^{-1}. The barrier associated with the non-polar DA reaction between Cp **1** and ethylene **2** is *ca.* 4 kcal mol^{-1} lower in energy than that for the DA reaction between butadiene **8**/ethylene **2**, partly due to the constrained *s-cis* conformation of Cp **1**.

The presence of the phenyl substituent on the C1–C2 double bond of styrene **10** opens two stereoisomeric channels: the *endo* and the *exo*. For this comparative study, only the *endo* approach modes of the phenyl substituent over the diene system of Cp **1** have been studied. In addition, as for the DA reaction between Cp **1** and ethylene **2**, only the reactive channels characterized by the α angles of *ca.* 60 and −60 degrees have been considered (see Scheme 4).

The activation barriers associated with the one-step and stepwise mechanisms for the DA reaction between Cp **1** and styrene **10** are 20.7 (**TS2c**) and 28.2 (**TS21**) kcal mol^{-1}, respectively. Now, the stepwise mechanism *via* **TS21** is 8.5 kcal mol^{-1} more unfavorable than that the concerted mechanism *via* **TS2c**. The presence of the phenyl substituent in styrene **10** diminishes the barrier associated with **TS21**, and stabilizes the corresponding diradical intermediate **DR2** in *ca.* 9 kcal mol^{-1} as a consequence of a large stabilization of the radical center that is being developed on the C1 carbon atom of this ethylene derivative. This DA reaction is exothermic by −17.0 kcal mol^{-1}. This reaction is less exothermic than the DA reaction between **1** and **2** as a consequence of the lost of conjugation present in styrene **10**.

The geometries of the TSs associated with the one-step and stepwise DA reactions between Cp **1** and ethylene **2** or styrene **10**, respectively, are given in Fig. 2. At the concerted **TS1c**, the lengths of the two C–C forming bonds are 2.249 Å, while the length of the C2–C3 forming bond at **TS11** associated with the stepwise mechanism is 1.877 Å. At the diradical intermediate **DR1** the length of the C2–C3 bond is 1.574 Å. These lengths are similar to those found by Houk in the concerted and stepwise TSs associated with the DA reactions between butadiene **8** and ethylene **2**: 2.273 and 1.875 Å, respectively.[7b]

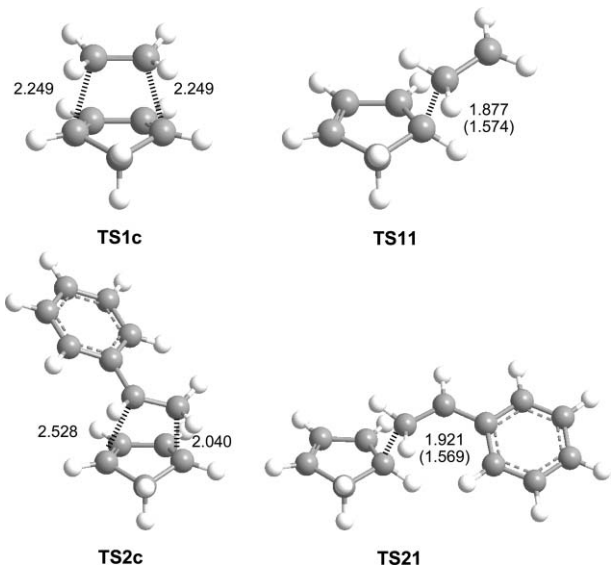

Fig. 2 (U)B3LYP/6-31G(d) transition structures associated with the one-step and stepwise pathways of the non-polar DA reactions between Cp **1** and ethylene **2** or styrene **10**. The C2–C3 bond lengths in **DR1** and **DR2** are given in parentheses. The lengths are given in Angstroms.

The presence of the phenyl substituent in styrene **10** breaks the symmetry of the concerted **TS1c**. The lengths of the two forming bonds at **TS2c** are 2.040 Å (C2–C3) and 2.528 Å (C1–C6). While the C2–C3 distance is shortened with respect to that at **TS1c**, the C1–C6 one is increased. Note that the C1 atom corresponds to a benzylic position, which allows for stabilization of the radical species. At **TS21**, which is associated with the stepwise mechanism, the length of the C2–C3 forming bond is 1.921 Å. This length is slightly larger than that found at **TS11** as a consequence of the stabilization of the corresponding diradical TS. Finally, in the diradical intermediate **DR2** the length of the C2–C3 bond is 1.569 Å.

In order to obtain a more precise idea of the bond-formation extension in the TSs, we resort to the bond order (BO) analysis.[15] In the concerted **TS1c**, the BO value of the two C–C forming bonds

is 0.36, while the BO value of the C2–C3 forming bond at **TS11** and **DR1** associated with the stepwise mechanism is 0.60 and 0.94, respectively. In the concerted **TS2c**, the BO values of the C2–C3 and C1–C6 forming bonds are 0.47 and 0.23. The C1–C(Ar) BO value at this TS, 1.13, points to some electron delocalization on the phenyl substituent. The presence of the phenyl substituent on styrene **10** breaks the symmetry of the C–C bond formation. The bond-formation at the benzylic position of **10** is more delayed. At **TS21** and **DR2**, associated with the stepwise mechanism, the BO values of the C2–C3 forming bonds are 0.56 and 0.95, respectively. In the biradical intermediates **DR1** and **DR2**, the C4–C5 and C5–C6 BO values, 1.46 and 1.47, point to a radical C4–C5–C6 allylic structure. Finally, the C1–C(Ar) BO values in **TS21**, 1.21, and **DR2**, 1.31, point to substantial electron delocalization on the phenyl substituent.

The electronic nature of these DA reactions was also evaluated analyzing the charge transfer (CT) at the TSs and at the diradical intermediates.[6] The natural charges at these species were shared between the Cp framework and the dienophile one, ethylene **2** or styrene **10**. The CT at the Cp fragment is: +0.03 e at **TS1c**, +0.02 e at **TS11** and 0.00 e at **DR1**, and +0.06 e at **TS2c**, +0.04 e at **TS21** and 0.00 e at **DR2**. There is an unappreciable CT from the Cp to the dienophile moieties. Note that at the diradical intermediates **DR1** and **DR2** the CT is null, in clear agreement with the non-polar biradical character of these stepwise processes.

The present comparative analysis between the non-polar DA reactions of Cp **1** with ethylene **2** or styrene **10**, indicates that the phenyl substituent present in **10** produces some significant changes at the asynchronous **TS2c**. While the energy results show that the activation barrier associated with the **TS2c** is 0.8 kcal mol^{-1} more unfavorable than that for concerted **TS1c**, the geometry and electronic structure of the asynchronous **TS2c** points to a larger stabilization of this TS. The stabilizing effect of the phenyl substituent can be explained by the larger stability of diradical intermediate **DR2** compared with **DR1**, about 9.0 kcal mol^{-1}. However, formation of CA **11** is 6.6 kcal mol^{-1} less exothermic than formation of CA **3**, as a consequence of the loss of conjugation present in styrene **10**. These results indicate two opposite effects on the activation energy associated with the asynchronous **TS2c**: a stabilizing effect associated with some electron-delocalisation on the TS, which can have some diradical character, and an unfavorable effect associated with the loss of conjugation of the C1–C2 double bond with the aromatic ring in the ground state of styrene **10**. The latter overcomes the stabilizing effect on **TS2c**, increasing the activation barrier slightly.

In order to evaluate these opposite effects, the two isodesmic reactions[16] shown in Scheme 5 were studied. Reaction (a) evaluates the stabilization on styrene **10** by conjugation of the C1–C2 double bond with the aryl system, while reaction (b) evaluates the stabilization of a benzylic radical relative to an alkylic one. The stabilization in styrene **10** by conjugation, which is estimated to be 6.9 kcal mol^{-1}, is in reasonable agreement with the diminishing of the exothermic character on the formation of the CA **11** relative to

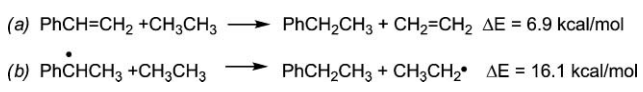

Scheme 5

that in the formation of CA **3**, 7.4 kcal mol^{-1}. On the other hand, the benzylic radical is estimated to be *ca.* 16 kcal mol^{-1} more stable than the primary alkylic radical. The energy difference between the two isodesmic reactions, 9.2 kcal mol^{-1}, is in reasonable agreement with the stabilization of **DR2** relative to **DR1**, 9.0 kcal mol^{-1}. That is, the loss of conjugation in styrene **10** is exceeded by the large stabilization of the corresponding benzylic radical intermediate formed in **DR2**. This larger radical stabilization can explain the asynchronicity found in **TS2c**, and in consequence, the diradical character of these concerted TSs (see later).

(b) Topological analysis of the ELF along the IRC of the concerted and stepwise pathways associated with the DA reaction between Cp 1 and ethylene 2

Recent studies devoted to cycloaddition reactions have shown the usefulness of the topological analysis of the ELF to understand the electron-reorganization along the reaction pathways associated with the C–C bond-formation processes.[13,14,17] The ELF basin populations of selected points on the IRC of the concerted and stepwise pathways for the Cp **1**/ethylene **2** DA reaction, including **TS1c**, **TS11** and the intermediate **DR1**, are displayed in Table 2 and Table 3. To reach this goal we have defined the **D** parameter along the reaction pathways, which correspond to the bond distance, in angstroms, between the carbon centers of Cp **1** and ethylene **2** (*e.g.* the C1–C6 and C2–C3 distances). For the concerted pathway, apart from the bonding pattern showed by both separated reagents, Cp **1** and ethylene **2**, four different phases, **I**–**IV**, are characterized and analyzed along the electronic rearrangement bonding. The attractor positions and the atom numbering of ELF for relevant points of the concerted pathway are shown in Fig. 3.

The ELF topological analysis of the attractors for Cp **1** shows three disynaptic attractors associated with the expected C–C single bond regions integrating to 1.98 e, 1.96 e and 2.17 e, and two disynaptic basins associated each one to the two C–C double bonds, whose electron density integrate to 3.47 e (*e.g.* V(C3,C4) and V′(C3,C4)) and 3.48 e (*e.g.*, V(C5,C6) and V′(C5,C6)). The picture for ethylene **2** also displays two disynaptic basins (*e.g.*, V(C1,C2) and V′(C1,C2)) that integrate to 3.46 e, associated with the C1–C2 double bond.

As both reagents approach each other along the phase **I**, 3.14 ≤ **D** ≤ 2.64 Å, the two disynaptic attractors associated to the C–C double bonds in Cp **1** are merged into each other to become one (*e.g.* V(C3,C4) and V(C5,C6)). In this first phase, the electronic populations of these basins decrease slightly compared with those observed in the isolated reagents. At the same interval, the electronic population in V(C4,C5) starts to increase from 2.37 e to 2.45 e. The electronic density integrated in the V(C3,C7) and V(C6,C7) basins is kept constant in phase **I**. When the molecules are closer to each other, as is shown in phase **II**, 2.54 ≤ **D** ≤ 2.24 Å, a similar ELF topological analysis to that found in phase **I** for the Cp framework is observed. A subtle electronic redistribution in the Cp **1** moiety is observed in the V(C3,C4), V(C4,C5) and V(C5,C6) basins; whereas the V(C3,C4) and V(C5,C6) basins decrease their population, the V(C4,C5) one increases it. The single bond character of V(C3,C7) and V(C6,C7) attractors is kept in phase **II**. In this phase, the two disynaptic basins associated to the C1–C2 double bond of ethylene **2** are merged into each

Table 2 ELF basin populations for the concerted pathway associated with the DA reaction between Cp **1** and ethylene **2**. A bonding between atoms in all phases is demonstrated by the standard Lewis representation; however, in the case of phase **III**, ellipses with points reflect the nonbonding electron density concentrated on the C atoms. See the text for details

D(Å)	Reagents	3.14	2.94	2.74	2.64	2.54	2.44	2.34	2.24	2.14	2.04	1.94	1.84	1. 74	1.64	1.56
Basins	**1 + 2**		**I**				**II**		**TS1c**		**III**			**IV**		**CA3**
V(C3,C4)	1.73	3.32	3.30	3.27	3.25	3.22	3.19	3.15	3.12	2.73	2.57	2.47	2.40	2.34	2.28	1.98
V′(C3,C4)	1.74	—	—	—	—	—	—	—	—	—	—	—	—	—	—	—
V(C4,C5)	2.17	2.37	2.39	2.43	2.45	2.49	2.56	2.62	2.71	2.87	3.05	3.17	3.26	3.32	2.25	1.82
V′(C4,C5)	—	—	—	—	—	—	—	—	—	—	—	—	—	—	—	1.73
V(C5,C6)	1.74	3.33	3.32	3.28	3.26	3.23	3.20	3.17	3.12	2.76	2.57	2.46	2.38	2.32	2.25	1.98
V′(C5,C6)	1.74	—	—	—	—	—	—	—	—	—	—	—	—	—	—	—
V(C3,C7)	1.98	1.98	1.99	1.99	1.99	1.97	1.99	1.97	1.98	1.95	1.95	1.94	1.92	1.90	1.88	1.82
V(C6,C7)	1.96	1.98	1.98	1.98	1.98	1.98	1.98	1.98	1.97	1.94	1.94	1.94	1.92	1.90	1.89	1.82
V(C3)	—	—	—	—	—	—	—	—	—	0.34	0.41	0.48	—	—	—	—
V(C6)	—	—	—	—	—	—	—	—	—	0.34	0.41	0.47	—	—	—	—
V(C2,C3)	—	—	—	—	—	—	—	—	—	—	—	—	1.01	1.12	1.23	1.80
V(C1,C6)	—	—	—	—	—	—	—	—	—	—	—	—	1.04	1.17	1.30	1.80
V(C1,C2)	1.73	1.73	1.72	1.70	1.73	3.30	3.30	3.32	3.33	2.76	2.62	2.50	2.40	2.31	2.23	1.85
V′(C1,C2)	1.73	1.62	1.62	1.62	1.60	—	—	—	—	—	—	—	—	—	—	—
V(C1)	—	—	—	—	—	—	—	—	—	0.30	0.37	0.43	—	—	—	—
V(C2)	—	—	—	—	—	—	—	—	—	0.30	0.38	0.44	—	—	—	—

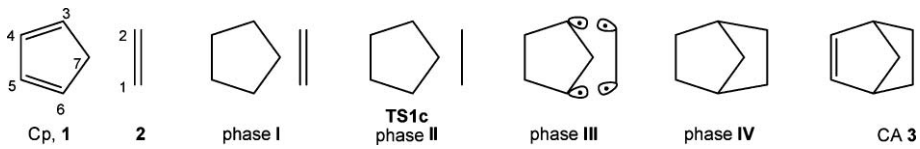

Table 3 ELF basin populations for the stepwise pathway associated with the DA reaction between Cp **1** and ethylene **2**. A bonding between atoms in all phases is demonstrated by the standard Lewis representation; however, in the case of phase **IV** and **DR1**, ellipses with points reflect the nonbonding electron density concentrated on the C atoms. See the text for details

D(Å)	Reagents	3.11	2.80	2.47	2.28	2.18	2.08	1.98	1.88	1.85	1.77	1.67	1. 60	1.59
Basins	**1 + 2**			**I**			**II**	**III**	**TS11**	**IV**	**V**		**VI**	**DR1**
V(C3,C4)	1.73	1.71	1.75	1.78	1.78	1.78	1.76	3.36	3.30	3.30	3.26	3.20	3.17	3.16
V′(C3,C4)	1.74	1.78	1.73	1.69	1.97	1.66	1.65	—	—	—	—	—	—	—
V(C4,C5)	2.17	2.17	2.18	2.20	2.23	2.26	2.31	2.41	2.51	2.51	2.61	2.89	2.95	2.97
V(C5,C6)	1.74	1.68	1.69	1.65	1.66	1.65	3.27	3.24	2.72	2.72	2.56	2.25	2.17	2.15
V′(C5,C6)	1.74	1.76	1.73	1.72	1.67	1.65	—	—	—	—	—	—	—	—
V(C3,C7)	1.98	1.96	1.99	1.97	1.97	1.97	1.98	1.99	2.00	2.00	2.00	2.00	2.01	2.01
V(C6,C7)	1.96	1.98	1.99	2.00	2.01	2.00	1.99	1.96	1.92	1.92	1.89	1.86	1.84	1.84
V(C3)	—	—	—	—	—	—	—	—	0.52	0.52	—	—	—	—
V(C2,C3)	—	—	—	—	—	—	—	—	—	—	1.18	1.41	1.54	1.56
V(C1,C2)	1.73	1.74	1.74	1.72	1.72	1.72	1.74	3.43	3.09	3.09	2.94	2.41	2.36	2.29
V′(C1,C2)	1.73	1.73	1.72	1.74	1.73	1.71	1.69	—	—	—	—	—	—	—
V(C2)	—	—	—	—	—	—	—	—	0.35	0.35	—	—	—	—
V(C1)	—	—	—	—	—	—	—	—	—	—	—	—	—	0.05
V′(C1)	—	—	—	—	—	—	—	—	—	—	—	0.42	0.42	0.41

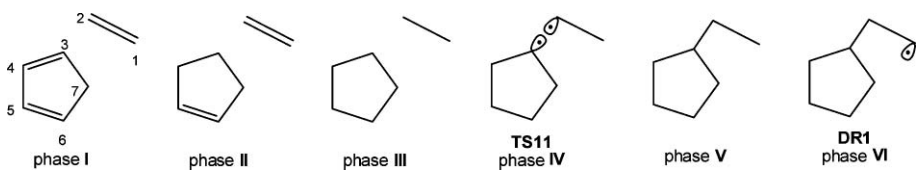

other to become V(C1,C2), whose electron density integrates to 3.30 e. At the end of phase **II** is located the concerted **TS1c** (**D** = 2.24 Å).

In phase **III**, 2.14 Å ≤ **D** ≤ 1.94 Å, it may be seen drastic changes in the original basin of attractors. Four monosynaptic basins (*e.g.* V(C1), V(C2), V(C3) and V(C6)) appear at C1 and C2 carbon atoms of ethylene **2** and at the C3 and C6 terminal carbons of Cp **1**. The ELF analysis shows a population of 0.30 e associated to each basin of the two carbon atoms of the ethylene **2** fragment (*e.g.* V(C1) and V(C2)) and 0.34 e for each basin associated to the terminal carbon atoms in Cp **1** ((*e.g.* V(C3) and V(C6)). The electronic population associated to basins V(C3,C4) and V(C5,C6) decreases, whereas that associated to the V(C4,C5) one increases in this phase. At **D** = 1.94 Å, it can be observed that the monosynaptic basins associated to all terminal carbon atoms increase 0.1e compared to those seen at **D** = 2.14 Å. Even though the population of V(C3,C7) and V(C6,C7) basins decrease slightly, note that it is almost kept constant in phase **III**. The electronic population in ethylene **2** decreases in this interval. Similar ELF topological rearrangement was recently found at the phase **V**, **D** = 2.19 Å, of the concerted pathway associated with the DA reaction between butadiene **8** and ethylene **2**.[13]

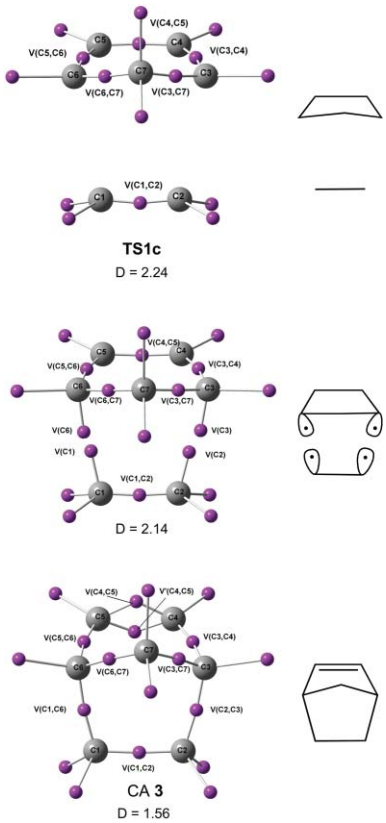

Fig. 3 Spatial localization of the maximum (*e.g.* attractors) of the ELF for relevant points on the IRC for the one-step pathway of the non-polar DA reaction between Cp **1** and ethylene **2**. Distances *D* are given in Angstroms. The corresponding Lewis structures are also shown. They do not include C–H bonds. Ellipses with points reflect the nonbonding electron density concentrated on the C atoms.

At the begining of the last phase **IV**, 1.84 ≤ **D** ≤ 1.56 Å, the four monosynaptic basins are merged into two new disynaptic V(C2,C3) and V(C1,C6) basins, which integrate *ca.* 1e, being this electron-reorganization associated with the formation of the two new C2–C3 and C1–C6 single bonds. Along this phase, the population of these basins increases until to reach a population of 1.80 e at CA **3**. Whereas the electronic population associated with the V(C3,C4) and V(C5,C6) basins, and the V(C3,C7) and V(C6,C7) basins assigned to C–C single bonds decrease to 1.98 e and 1.82 e, respectively, two new attractors associated with the C4–C5 double bond, namely V(C4,C5) and V′(C4,C5), which integrate to a population of 3.55 e, appear at CA **3**.

In summary, the topological analysis of the ELF for the concerted pathway associated with the DA reaction between Cp **1** and ethylene **2** provides further evidence for a *pseudo-diradical* character of the Cp and ethylene frameworks when the structures cross phase **III**, 2.14 ≤ **D** ≤ 1.94 Å, which collapse to the formation of the two new C–C single bonds at the beginning of phase **IV** to yield the CA **3**. Note that the synchronous **TS1c** structure is located at the end of phase **II**, and this structure does not show any relevant changes on the electron-reorganization. This picture for the concerted pathway of the DA reactions between Cp **1** and ethylene **2** is similar to that obtained for the concerted pathway associated with the DA reaction between 1,3-butadiene **8** and ethylene **2**, which was rationalized within the catastrophe theory distinguishing seven phases and characterizing 10 catastrophes.[13] The topological analysis of the ELF for these concerted DA reactions indicates that the electron-reorganization along the C–C bond formation does not show *changing in bonding on a close curve* as is proposed in the *pericyclic* model.[9] On going from the reagents to the concerted TSs, the high activation energies demanded to reach these non-polar TSs can be associated with the changes in the π system of both the diene and dienophile to reach *pseudo-diradical* structures.[18] Once these states are reached, the reactions fall down to formation of CAs toward a thermodynamically favored C–C bond formation process.

Consequently, in order to gain deeper insights about the electronic reorganization in the stepwise mechanism of the DA reaction between Cp **1** and ethylene **2**, we have performed a topological analysis of ELF along selected points of the IRC of the first step associated with formation of the radical intermediate **DR1**. For this step, six phases are characterized and analyzed, **I**–**VI** (see Table 3). The attractor positions and the atom numbering of ELF for relevant points of this step are shown in Fig. 4.

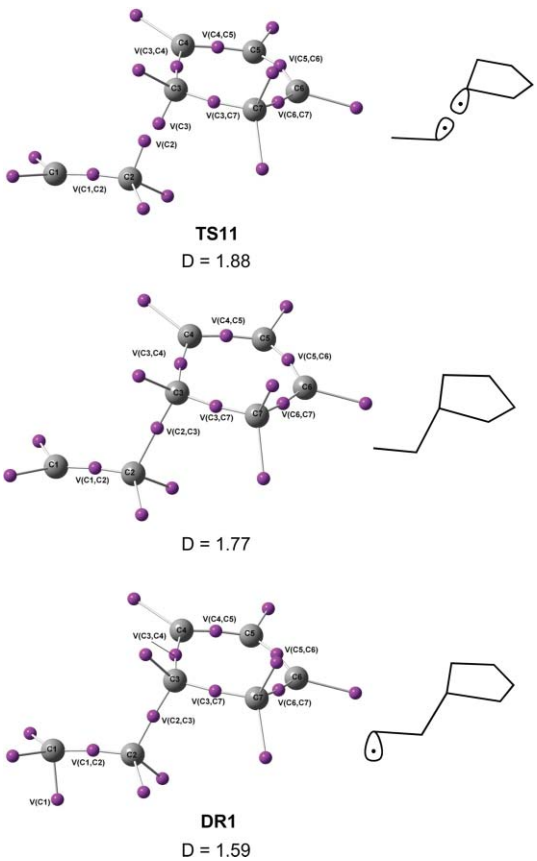

Fig. 4 Spatial localization of the maximum (*e.g.* attractors) of the ELF for relevant points on the IRC for the first step of the stepwise pathway of the non-polar DA reaction between Cp **1** and ethylene **2**. Distances **D** are given in angstroms. The corresponding Lewis structures are also shown. They do not include C–H bonds. Ellipses with points reflect the nonbonding electron density concentrated on the C atoms.

Along phase **I**, 3.11 ≤ **D** ≤ 2.18 Å, the population associated with disynaptic V(C3,C7) basin decreases slightly, whereas the population associated with the V(C6,C7) basin increases slowly. Again, subtle changes in the electron population associated

with V(C3,C4), V(C4,C5) and V(C5,C6) basins are observed in this region. Four disynaptic attractors for V(C3,C4) (and the corresponding V′(C3,C4)) and V(C5,C6) (and the corresponding V′(C5,C6)) of the Cp **1** moiety integrate to 3.44 e and 3.30 e, respectively. For the ethylene fragment the total electronic population associated with the two V(C1,C2) and V′(C1,C2) disynaptic attractors decrease slightly. Phases **II** and **III** are very short. In phase **II**, 2.18 ≤ **D** ≤ 2.08 Å, the picture is similar to that observed in phase **I**, but the two disynaptic attractors associated with the C5–C6 double bond are merged into one (*e.g.* V(C5,C6)), which accounts for 3.27 e. In phase **III**, a similar topological behavior is observed for the two original attractors associated with the C3–C4 double bond of Cp **1**, which are merged into one (*e.g.* V(C3,C4)), integrating to 3.36 e and the two original attractors associated with the C1–C2 double bond of ethylene **2**, which are merged into one (*e.g.* V(C1,C2)), integrating to 3.43 e. Phase **IV**, 1.88 ≤ **D** ≤1.85 Å, contains two points along the IRC including the **TS11** (**D** = 1.88 Å). An interesting aspect to emphasize is the electron-reorganization at the **TS11** and near to that. One monosynaptic attractor appears on the C3 carbon atom at the Cp **1** moiety (0.52 e), and another one on the C2 carbon atom of the ethylene **2** fragment (0.35 e). Note that the electron populations decrease slightly in regions associated with the C3–C4 bond, and strongly in region associated with C5–C6 and C1–C2 bonds (*e.g.* V(C5,C6) and V(C1,C2)) under the formation of the V(C3) and V(C2) monosynaptic basins. It is worth mentioning that in the short phase **V**, **D** = 1.77 Å, the V(C2) and V(C3) monosynaptic basins merge into one disynaptic basin V(C2,C3), with 1.18 e, which is associated with the formation of the new C2–C3 single bond in **DR1**. The electron population of the V(C3,C4), V(C5,C6), V(C6,C7) and V(C1,C2) basins decreases whereas the population of the V(C4,C5) basin begins to increase to reach double bond character in the last phase **VI**. It can be observed in this phase a large enhancement of the electron population in the C2–C3 region of the single bond, as well as in the region associated with C4–C5 double bond until to reach **DR1**. As a result, a decrease in the population of V(C3,C4), V(C4,C5), V(C4,C7) and V(C1,C2) attractors is observed as a consequence of the above electronic rearrangements. Note that in phase **VI**, 1.67 ≤ **D** ≤ 1.59 Å, a V(C1) monosynaptic basin (0.45 e) is formed on the terminal ethylene C1 carbon atom. The ELF topological analysis reveals in this case the formation of the **DR1** structure as a diradical species having one electron delocalized on the C(H)4–C(H)5–C(H)6 framework of Cp **1**, and another one localized mainly at the terminal carbon of the ethylene **2** framework.

The ELF analysis seems to be consistent with the fact that both concerted and the first step of the stepwise mechanism of the DA reaction between Cp **1** and ethylene **2** can be rationalized under a common electron-reorganization. The high energies associated with these pathways can be related to the electron-reorganization demanded to reach the formation of the *pseudo-diradical* structures in the Cp and ethylene frameworks, which couple to form the new C–C single bonds at **D** ≈ 1.84 Å at the concerted pathway and **D** ≈ 1.80 Å at the stepwise one. The coupling of the *pseudo-diradical* frameworks at the first step of the stepwise pathway with formation of the diradical intermediate **DR1** is energetically disfavored by 15.0 kcal mol^{-1} relative to the simultaneous double diradical coupling in the concerted pathway. This large energy difference involved in both electron-reorganizations allows discarding the stepwise mechanism as a route for the non-polar DA reaction between Cp **1** and ethylene **2**.

In order to test the formation of *pseudo-diradical* structures along the IRC associated with the one-step mechanisms of non-polar DA reactions, we additionally have studied some relevant points of the one-step and stepwise mechanisms of the DA reaction between Cp **1** and styrene **10** to comparative analysis.

(c) Topological analysis of the ELF of some relevant points on the IRC of the one-step and stepwise pathways associated with the DA reaction between Cp 1 and styrene 10

The electronic populations on the main ELF basin attractors along the selected points are summarized in Table 4, including the **TS2c** and CA **11** for the one-step pathway, and **TS21** and **DR2** as the intermediate in the stepwise one. The attractor positions and the atom numbering are depicted in Fig. 5.

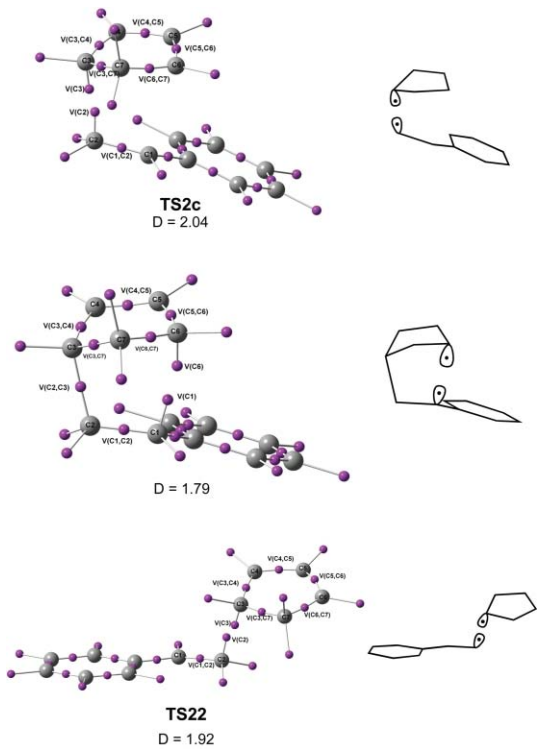

Fig. 5 Spatial localization of the maximum (*e.g.* attractors) of the ELF for relevant points on the IRC for the one-step and step-wise pathways of DA reaction between Cp **1** and styrene **10**. Distances **D** are given in Angstroms. The corresponding Lewis structures are also shown. They do not include C–H bonds. Ellipses with points reflect the non-bonding electron density concentrated on the C atoms.

At styrene **10**, both attractors, V(C1,C2) and V′(C1,C2), show similar populations to those observed in ethylene **2**. As Cp **1** and styrene **10** approach each other to achieve **TS2c** through the one-step pathway, two monosynaptic attractors V(C3) and V(C2) are formed on the C3 carbon atom of the Cp fragment and on the C2 carbon atom of the styrene one, which integrate to 0.41 e and 0.39 e. The formation of attractors just on one side of the C2–C3 forming bond region may be traced back to the presence of the phenyl group on the C1 carbon atom of styrene, which allows for a favorable delocalization of the C1 *pseudo-radical* on the phenyl

Table 4 ELF basin populations for some selected points of the one-step and stepwise pathways associated with the DA reaction between Cp **1** and styrene **10**. A bonding between atoms at selected points is demonstrated by the standard Lewis representation; however, in the case of **TS2c** and **TS21**, ellipses with points reflect the nonbonding electron density concentrated on the C atoms. See the text for details

D(Å)	Reagents	2.04	1.79	1.59	1.92	1.84	1.57
Basins	**1** + **10**	**TS2c**		CA**11**	**TS21**		**DR2**
V(C3,C4)	1.74	2.72	2.22	1.98	2.73	2.59	2.13
V′(C3,C4)	1.74	—	—	—	—	—	—
V(C4,C5)	2.17	2.68	3.18	1.81	2.49	2.58	2.96
V′(C4,C5)	—	—	—	1.72	—	—	—
V(C5,C6)	1.73	3.12	2.51	2.00	3.30	3.27	3.15
V′(C5,C6)	1.74	—	—	—	—	—	—
V(C3,C7)	1.96	1.93	1.87	1.83	1.93	1.91	1.86
V(C6,C7)	1.98	2.00	1.98	1.82	2.00	2.00	2.01
V(C3)	—	0.41	—	—	0.48	—	—
V(C6)	—	—	0.43	—	—	—	—
V(C2,C3)	—	—	1.39	1.80	—	1.12	1.66
V(C1,C6)	—	—	—	1.78	—	—	—
V(C1,C2)	1.75	2.93	2.28	1.87	2.94	2.76	2.14
V′(C1,C2)	1.74	—	—	—	—	—	—
V(C1)	—	—	0.43	—	—	—	—
V(C2)	—	0.39	—	—	0.37	—	—

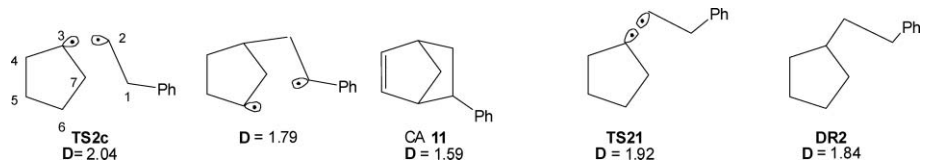

ring. Note that the C6 *pseudo-radical* is also delocalized in the C4–C5–C6 allylic framework. At **D** = 1.79 Å, the V(C3) and V(C2) basins disappear and a new disynaptic attractor emerges in the C2–C3 region bond, V(C2,C3) showing a population of 1.39 e, whereas two new monosynaptic attractors V(C1) and V(C6) are formed on C1 atom carbon of styrene **10** and the C6 carbon of Cp **1**, integrating to 0.43 e each one. These new monosynaptic basins allow for the formation of the second single bond in a subsequent step. When CA **11** is formed, the disynaptic basins associated with the new C1–C6 and C2–C3 single bonds reach a population of 1.80 e, and the population associated with C4–C5 bond region increases to reach the formation of two disynaptic attractors, the V(C4,C5) and the V′(C4,C5), associated with the double C4–C5 bond.

For the stepwise pathway, the ELF topological analysis for **TS21** displays a very similar pattern to that found for **TS2c**, *i.e.*, two monosynaptic attractors are found on the C3 and C2 terminal carbon atoms of the Cp **1** and styrene **10**, whereas the population associated with the C5–C6 bond begins to decrease. Then, at **D** = 1.84 Å, the two monosynaptic basins are merged into one disynaptic V(C2,C3) integrating 1.12 e, while the population in the C1–C2 single bond region begins to decrease and that of the C4–C5 bond region is increases. Finally, at the **DR2** intermediate the population of the C2–C3 region bond increases to 1.66 e with an increase of the population on V(C4,C5) and a slightly decreasing in the electronic population of the V(C5,C6).

Summarizing, the ELF topological analysis for **TS2c** associated with the one-step pathway and that for **TS21** associated with the stepwise one of the non-polar DA reaction between Cp **1** and styrene **10** shows very similar electron-reorganization patterns; both TSs are associated with the formation of the C2–C3 single bond. While in the one-step pathway, once the C2–C3 single bond is formed begins the formation of the C1–C6 one, in the stepwise pathway a rotation of the new C2–C3 single bond is required in order to achieve the formation of the second single bond. The presence of the phenyl substituent on styrene **10** breaks the symmetry found at the concerted **TS1c** as a consequence of some delocalization of the electron-density of the corresponding *pseudo-diradical* structure on the phenyl substituent. This pattern produces a remarkable change in the geometry and in the synchronicity of the bond formation at **TS2c**. These analyses follow the same pattern as that found in the non-polar DA reactions between 1,3-butadiene **8** and ethylene **2**, which was rationalized through the catastrophe theory together with the electron localization function.[13] Going to the unfavorable TSs associated with non-polar DA reactions, an electron-reorganization associated with the break of the three π bonds is needed to reach the formation of the *pseudo-diradical* structures, which couple to form the new C–C single bonds at **D** ≈ 1.8 Å.

Conclusions

The topological analysis of the ELF for the concerted and the first step of the stepwise pathways associated with the DA reaction between Cp **1** and ethylene **2** suggests that the concerted and stepwise mechanisms take place under a common electron-reorganization. The high energy barriers of the concerted and stepwise TSs are related to the electron-reorganization associated with the break of the π bonds of reagents required to reach the formation of the *pseudo-diradical* structures at the Cp and ethylene frameworks. At **D** ≈ 1.80 Å, these *pseudo-diradical* species couple to form the new C–C single bonds. The coupling in the stepwise pathway with formation of the diradical intermediate **DR1** is energetically disfavored relative to the simultaneous double diradical coupling in the concerted pathway. The energetic difference involved in

both electron-reorganizations allows one to rule out the stepwise mechanism for the non-polar DA reaction between Cp **1** and ethylene **2**.

An analysis of the asynchronous **TS2c** involved in the one-step pathway of the DA reaction between Cp **1** and styrene **10** indicates that the asynchronicity of the bond formation is associated with a radical stabilization of the corresponding **TS2c** promoted by the presence of the phenyl substituent on the ethylene framework. This behavior, which does not change the non-polar character of the DA reaction, allows for asserting that the one-step pathways of these non-polar DA reactions have a similar electron-reorganization pattern associated with the coupling of two *pseudo-diradical* frameworks formed by unfavorable π bond breaking processes.

From the ELF topological analysis of the changes of bonding along the reaction coordinate associated with the one-step pathways of these non-polar DA reactions, we can conclude that they do not follow a cyclic electron-reorganization pattern as proposed in the known *pericyclic* model, but a symmetric electron-reorganization in which the three π bonds present in reagents are broken in an unfavorable process to reach *pseudo-diradical* species, which couple to form the new single bonds. The presence of the phenyl substituent on styrene breaks the symmetry of the breaking and forming bonds by a stabilization of the corresponding *pseudo-diradical* species.

Methods and computational details

All calculations were carried out with the Gaussian 03 suite of programs.[19] DFT calculations were carried out using the B3LYP[20] exchange–correlation functionals, together with the standard 6-31G(d) basis set.[21] For the stepwise pathways involving diradical intermediates, the unrestricted formalism (UB3LYP) was employed. The optimizations were carried out using the Berny analytical gradient optimization method.[22] The stationary points were characterized by frequency calculations in order to verify that TSs have one and only one imaginary frequency. The IRC[23] paths were traced in order to check the energy profiles connecting each TS to the two associated minima of the proposed mechanism using the second order González-Schlegel integration method.[24] The electronic structures of stationary points were analyzed by the NBO method[25] and the topological analysis of the ELF.[11] The ELF study was performed with the TopMod program[26] using the corresponding monodeterminantal wavefunctions of the selected structures of the IRC.

The electron localization function ELF, $\eta(\mathbf{r})$,[27] is a relative measure of the same spin pair density local distribution, *i.e.* the Pauli repulsion. High values of the ELF are associated with high probability regions for electron pairing in the spirit of Lewis structures. The analysis and interpretation of ELF, originally introduced in the context of monodeterminantal wavefunctions, have also been recently generalized to the treatment of correlated wavefunctions.[28] Comprehensive explanations concerning the topological analysis of ELF nomenclature have been presented elsewhere and we have here focus on the relevant details necessary for our current application. The analysis of the gradient field or topology of ELF[29] renders a partition of the molecular space into non-overlapping volumes or *basins* that could be associated with entities and concepts of chemical significance as atomic cores and valence regions (*e.g.*, bonds or lone pairs). Valence basins are in turn classified depending of the number of core basins with which they share a boundary, (*i.e.*, the so-called synaptic order).[29a,b] A complete population analysis can be performed based on the integration of the one- and two-electron density probabilities in the ELF basins. This technique indeed provides a powerful quantitative population analysis. In such context, the average basin population in basin i is the result of integrating the electron density $\rho(\mathbf{r})$ in such region, $N_i = \int_i \rho(\mathbf{r})d\mathbf{r}$. Variances and delocalization indices can be also defined. The population analysis performed within the ELF basins has been found to be a useful tool to rationalize the *electron delocalization* in molecular systems,[30] giving a deeper insight into the nature of the chemical bond in a variety of stationary and reacting systems.[17]

Acknowledgements

We are grateful to the Spanish Government (project CTQ2009-11027/BQU), and the Fondecyt projects under contract Nos. 1100278 and 1100277. P. P. and E. Ch. also thank the Universidad Andrés Bello (UNAB) for support through projects DI 35-10/R and 03-09/R, respectively.

References

1 (*a*) W. Carruthers, *Some Modern Methods of Organic Synthesis*, Cambridge University Press, Cambridge, 1978; (*b*) W. Carruthers, *Cycloaddition Reactions in Organic Synthesis*, Pergamon, Oxford, 1990.
2 O. Diels and K. Alder, *Justus Liebigs Ann. Chem.*, 1928, **460**, 98.
3 K. Fukui, *Molecular Orbitals in Chemistry, Physics and Biology* ,New York, 1964.
4 (*a*) H. Eyring and M. Z. Polanyi, *Phys. Chem. Abt. B*, 1931, **12**, 279; (*b*) H. Eyring, *Chem. Rev.*, 1935, **17**, 65–77; (*c*) K. J. Laidler and M. C. King, *J. Phys. Chem.*, 1983, **87**, 2657–2664.
5 (*a*) P. Geerlings, F. De Proft and W. Langenaeker, *Chem. Rev.*, 2003, **103**, 1793–1873; (*b*) D. H. Ess, G. O. Jones and K. N. Houk, *Adv. Synth. Catal.*, 2006, **348**, 2337–2361.
6 L. R. Domingo and J. A. Sáez, *Org. Biomol. Chem.*, 2009, **7**, 3576–3583.
7 (*a*) K. N. Houk, J. Gonzalez and Y. Li, *Acc. Chem. Res.*, 1995, **28**, 81–90; (*b*) E. Goldstein, B. Beno and K. N. Houk, *J. Am. Chem. Soc.*, 1996, **118**, 6036–6043.
8 A. Wassermann, *J. Chem. Soc.*, 1935, 828–839.
9 R. B. Woodward and R. Hoffmann, *Angew. Chem., Int. Ed. Engl.*, 1969, **8**, 781.
10 X. Krokidis, S. Noury and B. Silvi, *J. Phys. Chem. A*, 1997, **101**, 7277–7282.
11 (*a*) A. Savin, A. D. Becke, J. Flad, R. Nesper, H. Preuss and H. G. Vonschnering, *Angew. Chem., Int. Ed. Engl.*, 1991, **30**, 409–412; (*b*) A. Savin, R. Nesper, S. Wengert and T. F. Fassler, *Angew. Chem., Int. Ed. Engl.*, 1997, **36**, 1808–1832.
12 R. Thom, *Stabilite Structurelle et Morphogenese*, Intereditions, Paris, 1972.
13 S. Berski, J. Andres, B. Silvi and L. R. Domingo, *J. Phys. Chem. A*, 2003, **107**, 6014–6024.
14 L. R. Domingo, E. Chamorro and P. Pérez, *Lett. Org. Chem.*, 2010, **7**, 432–439.
15 K. B. Wiberg, *Tetrahedron*, 1968, **24**, 1083–1096.
16 F. A. Carey and R. J. Sundberg, *Advanced Organic Chemistry. Part A: Strucutre and Mechanisms*, New York, 2008.
17 (*a*) V. Polo, L. R. Domingo and J. Andres, *J. Phys. Chem. A*, 2005, **109**, 10438; (*b*) S. Berski, J. Andres, B. Silvi and L. R. Domingo, *J. Phys. Chem. A*, 2006, **110**, 13939–13947; (*c*) L. R. Domingo, M. T. Picher, P. Arroyo and J. A. Saez, *J. Org. Chem.*, 2006, **71**, 9319–9330; (*d*) V. Polo, L. R. Domingo and J. Andres, *J. Org. Chem.*, 2006, **71**, 754; (*e*) L. R. Domingo, M. T. Picher and P. Arroyo, *Eur. J. Org. Chem.*, 2006, 2570–2580; (*f*) L. R. Domingo, E. Chamorro and P. Pérez, *J. Org. Chem.*, 2008, **73**, 4615; (*g*) V. Polo, J. Andres, S. Berski, L. R. Domingo

and B. Silvi, *J. Phys. Chem. A*, 2008, **112**, 7128–7136; (*h*) G. Bentabed-Ababsa, A. Derdour, T. Roisnel, J. A. Sáez, P. Pérez, E. Chamorro, L. R. Domingo and F. Mongin, *J. Org. Chem.*, 2009, **74**, 2120–2133.

18 A similar *pseudo-diradical* structure has been found in the concerted non-polar [3+2] cycloaddition between the simplest azomethine ylide and ethylene.[14].

19 M. J. Frisch, G. W. Trucks, H. B. Schlegel, G. E. Scuseria, M. A. Robb, J. R. Cheeseman, J. A. Montgomery, Jr., T. Vreven, K. N. Kudin, J. C. Burant, J. M. Millam, S. S. Iyengar, J. Tomasi, V. Barone, B. Mennucci, M. Cossi, G. Scalmani, N. Rega, G. A. Petersson, H. Nakatsuji, M. Hada, M. Ehara, K. Toyota, R. Fukuda, J. Hasegawa, M. Ishida, T. Nakajima, Y. Honda, O. Kitao, H. Nakai, M. Klene, X. Li, J. E. Knox, H. P. Hratchian, J. B. Cross, V. Bakken, C. Adamo, J. Jaramillo, R. Gomperts, R. E. Stratmann, O. Yazyev, A. J. Austin, R. Cammi, C. Pomelli, J. Ochterski, P. Y. Ayala, K. Morokuma, G. A. Voth, P. Salvador, J. J. Dannenberg, V. G. Zakrzewski, S. Dapprich, A. D. Daniels, M. C. Strain, O. Farkas, D. K. Malick, A. D. Rabuck, K. Raghavachari, J. B. Foresman, J. V. Ortiz, Q. Cui, A. G. Baboul, S. Clifford, J. Cioslowski, B. B. Stefanov, G. Liu, A. Liashenko, P. Piskorz, I. Komaromi, R. L. Martin, D. J. Fox, T. Keith, M. A. Al-Laham, C. Y. Peng, A. Nanayakkara, M. Challacombe, P. M. W. Gill, B. G. Johnson, W. Chen, M. W. Wong, C. Gonzalez and J. A. Pople, *GAUSSIAN 03 (Revision C.02)*, Gaussian, Inc., Wallingford, CT, 2004.

20 (*a*) A. D. Becke, *J. Chem. Phys.*, 1993, **98**, 5648–5652; (*b*) C. Lee, W. Yang and R. G. Parr, *Phys. Rev. B: Condens. Matter*, 1988, **37**, 785–789.

21 W. J. Hehre, L. Radom, P. v. R. Schleyer, and J. A. Pople, *A. Ab initio Molecular Orbital Theory*, Wiley: New York, 1986.

22 (*a*) H. B. Schlegel, *J. Comput. Chem.*, 1982, **3**, 214–218; (*b*) H. B. Schlegel, *"Geometry Optimization on Potential Energy Surface," in Modern Electronic Structure Theory.*; Ed. Yarkony D.R.: Singapore, 1994.

23 K. Fukui, *J. Phys. Chem.*, 1970, **74**, 4161–4163.

24 (*a*) C. González and H. B. Schlegel, *J. Phys. Chem.*, 1990, **94**, 5523–5527; (*b*) C. González and H. B. Schlegel, *J. Chem. Phys.*, 1991, **95**, 5853–5860.

25 (*a*) A. E. Reed, L. A. Curtiss and F. Weinhold, *Chem. Rev.*, 1988, **88**, 899–926; (*b*) A. E. Reed, R. B. Weinstock and F. Weinhold, *J. Chem. Phys.*, 1985, **83**, 735–746.

26 S. Noury, X. Krokidis, F. Fuster and B. Silvi, *Comput. Chem.*, 1999, **23**, 597–604.

27 A. D. Becke and K. E. Edgecombe, *J. Chem. Phys.*, 1990, **92**, 5397.

28 E. Matito, B. Silvi, M. Duran and M. Sola, *J. Chem. Phys.*, 2006, **125**, 024301.

29 (*a*) B. Silvi, *J. Mol. Struct.*, 2002, **614**, 3–10; (*b*) A. Savin, B. Silvi and F. Colonna, *Can. J. Chem.*, 1996, **74**, 1088–1096; (*c*) B. Silvi and A. Savin, *Nature*, 1994, **371**, 683; (*d*) B. Silvi, *Phys. Chem. Chem. Phys.*, 2004, **6**, 256.

30 (*a*) B. Silvi, *Phys. Chem. Chem. Phys.*, 2004, **6**, 256; (*b*) R. F. W. Bader and M. E. Stephens, *J. Am. Chem. Soc.*, 1975, **97**, 7391; (*c*) X. Fradera, M. A. Bader and R. F. W. Austen, *J. Phys. Chem. A*, 1999, **103**, 304; (*d*) J. G. Angyan, M. Loos and I. Mayer, *J. Phys. Chem.*, 1994, **98**, 5244; (*e*) R. Ponec and M. Strnad, *Int. J. Quantum Chem.*, 1994, **50**, 43; (*f*) R. Ponec and F. Uhlik, *THEOCHEM*, 1997, **391**, 159.

